

KfK 4090

Juli 1986

Cluster Ion Acceleration with the Radiofrequency Quadrupole

H. O. Moser, A. Schempp
Institut für Kernverfahrenstechnik

Kernforschungszentrum Karlsruhe

111

KERNFORSCHUNGSZENTRUM KARLSRUHE

Institut für Kernverfahrenstechnik

KfK 4090

Cluster Ion Acceleration with the Radiofrequency Quadrupole

von

H.O. Moser und A. Schempp*)

KERNFORSCHUNGSZENTRUM KARLSRUHE GMBH, KARLSRUHE

*) Institut für Angewandte Physik der Universität Frankfurt/Main,
Robert-Mayer-Str. 2-4, D-6000 Frankfurt/Main.

Als Manuskript vervielfältigt
Für diesen Bericht behalten wir uns alle Rechte vor

Kernforschungszentrum Karlsruhe GmbH
Postfach 3640, 7500 Karlsruhe 1

ISSN 0303-4003

Clusterionen-Beschleunigung mit dem Radiofrequenz-Quadrupol

Zusammenfassung

Die Verwendung eines Radiofrequenz-Quadrupol-Beschleunigers zur Clusterionen-Beschleunigung wird untersucht mit den drei Zielsetzungen, die kinetische Energie der Clusterionen in den Bereich oberhalb 1 MeV zu bringen, die durch Stoßprozesse im Strahl verursachte Atomstromdichtegrenze hinauszuschieben, und die Komplexität und Kosten im Vergleich zur elektrostatischen Beschleunigung zu verringern.

Zwei Fälle werden betrachtet: erstens, die im Zusammenhang mit Grundlagenuntersuchungen interessierende Beschleunigung von Clusterionen im Massenbereich von 1 bis 100 amu von 5 auf 50 keV/Nukleon, zweitens, die für technische Anwendungen interessante Beschleunigung von Clusterionen im Massenbereich von 1 bis 10^6 amu von 5 meV auf 1 eV/Nukleon. Auf der Grundlage des Standes der Technik erweisen sich die jeweiligen resultierenden RFQ-Strukturen als machbar.

Cluster Ion Acceleration with the Radiofrequency Quadrupole

Abstract

In order to increase the kinetic energy of accelerated cluster ions in the range beyond 1 MeV, to widen the atomic flux density limit imposed by collision processes in the beam, and to reduce complexity and costs compared with electrostatic acceleration, the use of a radiofrequency quadrupole accelerator is examined. Two cases are considered: firstly, the acceleration of cluster ions in the mass range from 1 to 100 amu from 5 to 50 keV/nucleon which is interesting for basic research, secondly, the acceleration of cluster ions in the mass range from 1 to 10^6 amu from 5 meV to 1 eV/nucleon which is interesting for several technological applications. On the basis of the state of the art, the respective RFQ structures turn out to be feasible.

Introduction

Since its invention in 1969 /1/ and, in particular, since the successful experiments carried out at Los Alamos /2/, the RFQ has become the subject of research and development activities in many accelerator laboratories /3/. The RFQ presents a favorable alternative to the Cockcroft-Walton in the field of charged particles acceleration to MeV energies /3/. It is now widely used as a preinjector for various kinds of ions throughout the mass range from hydrogen up to heavy ions such as $^{238}\text{U}^{2+}$ /4/.

In this report, we examine its application to cluster ions. There is previous work on the linear acceleration of cluster ions. Gspann /5/ has studied the acceleration of cluster ion beams by a drift tube linear accelerator. Enjoji and coworkers /6/ are investigating a linear accelerator scheme characterized by equally spaced disc electrodes connected to a delay line in such a way that an accelerated potential wave is created. In spite of these theoretical works cluster ions have only been accelerated by electrostatic means /7/, so far.

The RFQ has the potential of improving some of the rather restrictive features of electrostatic acceleration. A final energy of e. g. 5 MeV is much more easily achieved, thus, the energy per nucleon at a given mass-to-charge ratio of the ion and vice versa can be appreciably higher. The longitudinal relative velocity spread due to the mass distribution of the cluster ions which, in the case of electrostatic acceleration, has been shown to cause a limitation on flux density /8/ is supposed to be significantly lowered beneath the value obtained with electrostatic acceleration. On the other hand, the radial focusing oscillations are an additional source of relative motion. However, according to our estimates, the resulting limit to flux density can be expected to be markedly higher than in the case of electrostatic acceleration. Furthermore, for a given final energy of 5 MeV, an RFQ is appreciably simpler, smaller and cheaper than an electrostatic accelerator. Compared to a conventional drift tube linac, the main advantage of an RFQ is its continuous transversal strong focusing. Thus, acceleration can start at very low particle velocities where a drift tube linac would be bulky and expensive.

There are numerous applications, in basic as well as in applied research, which can be supposed to benefit from cluster ion acceleration by RFQ. Chanut et al. /9/ investigated the secondary electron yield when hydrogen cluster ions impinge on solid surfaces. Thomas et al. /10/ worked on the ion-induced desorption by high-energy hydrogen clusters and on the application of these beams in microscopic surface analysis. Henkes and Pfeiffer /11/ and Chevallier et al. /12/ studied the disintegration of hydrogen cluster ions on their passage through gas targets. Obviously, an increase of the accessible mass range or of the final energy per nucleon together with the possibility to vary the mass of the cluster ion independently of its velocity would be highly desirable for this kind of studies.

Various, more technical applications of intense cluster-ion beams have been proposed or discussed. Haas et al. /13/ examined the refueling of plasmas by cluster-ion beams, Becker and co-workers /14/ investigated the production of negative hydrogen ions when cluster-ion beams of hydrogen interact with different targets, Be and Yano /15/ analyzed how the process of interaction between cluster ions and surfaces could be used to build powerful sources of H^- -beams, and, finally, Moser /16/ suggested an application to investigating the influence of the high atmosphere on space vehicles. These applications would benefit mostly from the possibility to accelerate intense beams to a given final velocity independent of the mass distribution of the beam particles. In the following sections, we shall analyze two typical cases, one characteristic of the basic research applications, the other of the technological applications.

Summarized description of RFQ and of cluster-ion beam sources

Several excellent descriptions of RFQs can be found in the literature /1,3/. For convenience, we shall summarize the basic features and symbols. To construct an RFQ, four electrodes are arranged symmetrically around a central z-axis (Fig.1). The electrodes are connected to an RF power supply in such a manner that, at a given time, adjacent electrodes have equal absolute values of potential, but with opposite sign. The distance between opposite electrodes is modulated periodically with z so that the path traveled by a particle during an RF period is equal to the

period of modulation $\beta\lambda$ where β is the relativistic beta and λ the RF wave length in free space. The modulation of adjacent electrodes is phase shifted by π . The basic formulae for the resulting focusing and accelerating fields are listed in Table 1. Figure 2 displays the coordinates and symbols used.

A source of hydrogen cluster ions is depicted schematically in Fig. 3. A beam of thermal-energy hydrogen clusters is produced from a supersonic nozzle source /17,18/. This beam travels through an ionizer where positive cluster ions are formed by electron impact /19/.

Table 1

Amplitudes of field components in an RFQ (cylindrical coordinates r, ψ, z)

$$E_r = -\frac{\chi V}{a^2} r \cos 2\psi - \frac{kAV}{2} I_1(kr) \cos kz$$

$$E_\psi = \frac{\chi V}{a^2} r \sin 2\psi$$

$$E_z = \frac{kAV}{2} I_0(kr) \sin kz$$

where the acceleration efficiency A and the focusing efficiency χ are given by

$$A = \frac{m^2 - 1}{m^2 I_0(ka) + I_0(mka)}$$

and

$$\chi = 1 - AI_0(ka),$$

respectively.

$(V/2) \sin(\omega t + \phi)$ RF voltage

I_0, I_1 Bessel functions

$k = 2\pi/\beta\lambda$ absolute value of wave vector of electrode distance modulation.

Cluster ion RFQ for basic research

In this case, the whole accelerator consists of an electrostatic pre-accelerator, a magnetic mass selector, and the RFQ. First, the cluster ions are preaccelerated to a kinetic energy of eU_a ; in the mass range of interest, e. g. from 1 to 100 nucleons, they are assumed to carry only a single charge. Then, they travel through the mass analyzer, and the selected species enters the RFQ. We require the bending radius of the mass analyzer to be fixed because of the rigid structure of the beam-line. To keep the RF supply simple, the RF frequency should be fixed, too. With the usual relations

$$\rho = Nm v / Ze B$$

and

$$Nm v^2 / 2 = Ze U_a$$

where

ρ	bending radius
N	number of nucleons per cluster ion
m	mass of a nucleon
v	velocity after preacceleration
Z	number of charges per ion (assumed $Z=1$)
e	elementary charge
B	magnetic flux density
U_a	acceleration voltage

we see that, when ρ and v are fixed, B/N and U_a/N are constant, too. Eliminating the velocity, we find

$$\rho = \sqrt{(2m/Ze)(U_a/N)} (N/B)$$

If N sweeps over the desired range

$$1 \leq N \leq N_{\max}$$

then U_a and B must scan simultaneously the ranges

$$U_{\min} \leq U_a \leq U_{\max}$$

and

$$B_{\min} \leq B \leq B_{\max},$$

respectively, in order to keep B/N and U_a/N constant.

For typical values of

$$\begin{aligned} N_{\max} &= 100 \\ U_{a\max} &= 5 \times 10^5 \text{ V} \\ B_{\max} &= 1 \text{ T} \end{aligned}$$

we can set up the following Table 2.

Table 2

N_{\max}	100
ρ/m	1.02
$v/10^5 \text{ m/s}$	9.8
ν_{RF}/MHz	69.2
B_{\min}/T	10^{-2}
$U_{a\min}/\text{V}$	5000
Energy gain	10
Velocity ratio	3.2

The kinetic energy per nucleon at the RFQ entrance is $eU_{a\min}$ which corresponds to the initial velocity quoted, the final kinetic energy per nucleon is assumed to be 50 keV and the modulation period of the RFQ electrodes at the entrance is set 1.4 cm.

Table 3 shows results from computer runs based on the parameters as required in Table 2.

Table 3

Example		I	II
Initial energy per nucleon	keV	5	
Final energy per nucleon	keV	50	
Maximum total energy	MeV	5	
Maximum number of nucleons per ion		100	
Geometry			
Length of accelerating structure	m	3.15	(5.43)
Clear aperture between electrodes	mm	6	
Number of cells		250	(357)
Initial length of cell ($\beta\lambda/2$)	cm	0.7	
Maximum modulation m		2	
Diameter of vacuum chamber	m	0.4	
RF system			
Frequency	MHz	69.2	
Peak voltage	kV	100	(50)
Power	kW	130	(40)
Duty cycle		0.1	(1)
Maximum field strength	MV/m	2.8	(1.7)
Beam			
Radial phase advance per cell		14°	(7°)
Initial longitudinal phase after shaper		-60°	(-40°)
Final longitudinal phase		-30°	
Final longitudinal phase spread		$\pm 27^\circ$	($\pm 17^\circ$)
Final relative energy spread	%	± 1	(± 0.7)
Transmission	%	50	(34)

Figures 4 and 5 display the energy, accelerating electric field strength, phase, and transmission versus the longitudinal position, for

both examples. The RFQ will have a 4-rod- $\lambda/2$ -structure which has been developed in Frankfurt /3/ (Fig. 1). Up to now, most of the RFQs have accelerated protons or light ions in a very short pulse mode. Especially for the acceleration of heavy ions or cluster ions at low frequencies with a high duty factor the 4-rod- $\lambda/2$ -structure promises to be efficient, compact and economical. In case of the lower electrode voltage of 50 kV, which is favorable for cw operation, two separate tanks will be used to keep down the length per tank for easier handling.

The data above have been calculated for a continuous, monoenergetic beam entering the RFQ. Thus, the whole longitudinal phase angle interval of 2π is filled with particles. A restriction of this interval greatly affects the energy spread at the expense of transmission. For example, taking $\pm 35^\circ$ initially results in a final energy spread of 0.8 %. Furthermore, the initial beam must not necessarily be monoenergetic. Even for an initial relative energy spread $\delta T/T$ of $\pm 10\%$ the final relative energy spread amounts to $\pm 1.7\%$, again for a continuous beam at the entrance. Thus, the RFQ acts as a velocity filter with lower transmission for larger velocity spreads at the entrance.

Cluster ion RFQ for intense beams

Previous work on the electrostatic acceleration of intense beams of hydrogen cluster ions showed a limit on the atomic flux density caused by the velocity distribution of the beam particles and the ensuing mutual collisions /8/. This limit can be expected to be extended by narrowing the width of the cluster-ion velocity distribution. Obviously, the injection scheme must differ from that of the basic research RFQ because it has to take into account that the fraction of the mass distribution accepted by the RFQ should be as large as possible and transmission should be high. In both references /5/ and /6/ special attention is paid to this question. For the following RFQ calculations we put aside this question and simply assume a continuous cluster-ion beam entering the RFQ at an ion velocity and mass-to-charge ratio of 1000 m/s and 10^6 , respectively. The acceleration is performed in two steps, from 5 meV to 0.1 eV and from 0.1 eV to 1 eV per nucleon, respectively. Table 4 contains the results for the first stage.

Table 4

Initial energy per nucleon	meV	5
Final energy per nucleon	eV	0.1
Maximum total energy	keV	100
Maximum number of nucleons per ion		10 ⁶
Geometry		
Length of accelerating structure	m	0.71
Clear aperture between electrodes	mm	6
Number of cells		93
Initial length of cell ($\beta\lambda/2$)	cm	0.5
Maximum modulation m		2
Diameter of vacuum chamber	m	0.5
RF system		
Frequency	kHz	100
Peak voltage	kV	20
Power	kW	30
Duty cycle		1
Maximum field strength	MV/m	0.65
Beam		
Radial phase advance per cell		67°
Initial longitudinal phase after shaper		-70°
Final longitudinal phase		-30°
Final longitudinal phase spread		$\pm 27^\circ$
Final relative energy spread	%	± 3.4
Transmission	%	94

Figure 6 shows the longitudinal dependence of the main parameters. On leaving the first RFQ section the beam has a longitudinal phase spread of 53.7°. Since the frequency in the second section is tripled, the phase spread goes up to 160° which fits well into the longitudinal

acceptance of the second stage. Table 5 and Fig. 7 contain the equivalent data for the second stage accelerating the 100 keV-beam to 1 MeV.

Table 5

Initial energy per nucleon	eV	0.1
Final energy per nucleon	eV	1.0
Maximum total energy	MeV	1.0
Maximum number of nucleons per ion		10^6
Geometry		
Length of accelerating structure	m	1.6
Clear aperture between electrodes	mm	6
Number of cells		132
Initial length of cell ($\beta\lambda/2$)	cm	0.7
Maximum modulation m		2
Diameter of vacuum chamber	m	0.5
RF system		
Frequency	kHz	300
Peak voltage	kV	50
Power	kW	30
Duty cycle		1
Maximum field strength	MV/m	1.28
Beam		
Radial phase advance per cell		16.4°
Initial longitudinal phase after shaper		-60°
Final longitudinal phase		-30°
Final longitudinal phase spread		$\pm 20^\circ$
Final relative energy spread	%	± 2.3
Transmission	%	100

For such frequencies, power supplies up to 30 kW are commercially available. There will be no cavity as for 20- 100 MHz, but the 4-rod- $\lambda/2$ -structure will look similarly. It can be directly supplied with the

voltages of 50 kV and 20 kV, respectively, via non-resonant one-step transformation of the generator power. Ferrite core transformers may be used.

Discussion

We now want to estimate the influence of the longitudinal and radial oscillations on the mutual collisions between beam particles and the subsequent gas production. The number of collisions, Z , a given cluster undergoes during acceleration, is given by

$$Z = n \cdot \sigma_c \cdot l$$

where n is the number density of the cluster ions in the beam, σ_c is the cross section for cluster-cluster collision, and l is the path traveled by the cluster considered in the rest frame of the beam. If there are two motions perpendicular to each other, each characterized by velocities v_t and v_l , respectively, the total velocity is given by $v_{tot} = (v_t^2 + v_l^2)^{1/2}$. v_l can be derived from the longitudinal relative energy spread $\delta E/E$ as computed by the program. We obtain

$$v_l = \sqrt{(E/2m)} \delta E/E.$$

In order to estimate the transverse velocity, we assume a sinusoidal transverse oscillation the frequency of which is given by the RF frequency times the phase advance. If r denotes the radial elongation, then

$$r(t) = r_{max} \sin((\omega \hat{\sigma}/2\pi)t + \psi_0.)$$

where

r_{max}	maximum transverse amplitude
ω	angular RF frequency
$\hat{\sigma}$	radial phase advance in radian
ψ_0	constant phase angle, which is not needed further.

The maximum transverse velocity follows from differentiation as

$$v_{t,max} = r_{max} \cdot v_{RF} \cdot \hat{\sigma}$$

Finally, l can be estimated by

$$l = v_{\text{tot}}L/v,$$

with L as the accelerator length and v as the mean velocity. The following Table 6 gives an idea of the orders of magnitude involved.

Table 6

	Basic research RFQ	Intense beams RFQ
Number of atoms/cluster	10 ²	10 ⁶
Cross-section for cluster- cluster collision σ_c/cm^2	7.5x10 ⁻¹⁴	3.5x10 ⁻¹¹
Atomic flux density/A ₀ /cm ²	10 ⁻³ *)	0.5 *)
Mean velocity v/m/s	2x10 ⁶	7400
Number density of clusters/cm ⁻³	3x10 ⁵	4.2x10 ⁶
Accelerator length L/m	5.4	2.3
Clear aperture 2r _{max} /mm	6	6
RF frequency ν_{RF} /MHz	69	0.3(0.1)
Final energy per nucleon E/eV	5x10 ⁴	1
Relative energy spread	±0.007	± 0.023
Radial phase advance $\hat{\sigma}$ /radian	0.12	0.29
Relative longitudinal velocity v_l /m/s	2.2x10 ⁴	318
Relative transverse velocity v_t /m/s	2.5x10 ⁴	261
Total relative velocity v_{tot} /m/s	3.3x10 ⁴	411
Rest frame path length l/m	0.09	0.13
Number of collisions per cluster Z	2x10 ⁻⁷	0.002

*) typical values as quoted in /8/.

In the case of the basic research RFQ, the number of collisions is so small that the interaction with the ever present background gas will predominate. Background gas pressures of the order of 10⁻⁷ mbar should be sufficient. If one takes into account space charge the maximum ion current exceeds 4 mA.

In the case of the intense beams RFQ, the number of collisions is not sufficiently low to be neglected a priori. In order to assess its

meaning, we go back to the mechanism of gas production in an accelerated beam as discussed in /8/. There, the collisions of cluster ions among themselves and with gas particles within the beam serve as a source for the production of a gas cloud moving at beam velocity and characterized by approximately the same velocity spread as the cluster ions. It is the interaction of this gas with the cluster ions which is thought to lead, above a certain density limit, to an unstable growth of the gas number density, if the energy belonging to the relative motion is sufficiently high. This energy, however, is only 1.8 meV per H₂ molecule as follows from the relative velocity of 411 m/s quoted above. Thus, no additional background gas can be produced taking into account the sublimation enthalpy of 7.6 meV per H₂ molecule. As a consequence, it is justified to expect a marked reduction of the influence of mutual collisions by acceleration of intense beams of cluster ions with an RFQ instead of with an electrostatic accelerator. It is, however, important to approach a 100 % transmission in this case because the relative velocity between the cluster ions and particles produced by cluster impact on electrodes and other structures may amount to several 10³ m/s, and because collisions will then lead to further gas production. Obviously, the RFQ structure lends itself to a pumping which is distributed along the accelerator, e.g. by cryopumps or Ti sublimation pumps, and the structure has a reasonable transparency. The space-charge limited ion current amounts to about 10 μA.

To increase the total flux with fixed flux density, an array of parallel RFQ systems could be used according to an idea by Paul and coworkers /20/ and using RFQ structures developed by the Frankfurt group /21/.

Finally, an order of magnitude estimate of the cost of such RFQ systems gives DM 1 million.

References

- /1/ I.M. Kapchinskii, V.A. Teplyakov, Prib. Tekh. Eksp., No. 2, 19(1970).
- /2/ K.R. Crandall, R.H. Stokes, J.E. Stovall and D.A. Swenson, IEEE Trans. Nucl. Sci. NS-26, 3469(1979).
- /3/ H. Klein, IEEE Trans. Nucl. Sci. NS-30, 3313(1983); A. Schempp, P. Junior, H. Klein, M. Daehne, M. Ferch, K. Langbein, N. Zoubek, IEEE Trans. Nucl. Sci. NS-30, 3536(1983); S.O. Schriber, IEEE Trans. Nucl. Sci. NS-32, 3134(1985).
- /4/ R.W. Mueller, GSI 79-7, 1979; R.W. Mueller, U. Kopf, J. Bolle, S. Arai, P. Spaedtke, GSI 84-11, p. 77.
- /5/ J. Gspann, unpublished, 1971; J. Gspann, submitted to Journal of Physical Chemistry.
- /6/ H. Enjoji, H. Suzuki, M. Kawaguchi, 13th Symp. on Fusion Technology, Varese, Italy, 1984; H. Suzuki, H. Enjoji, M. Kawaguchi, T. Noritake, Jap. J. Appl. Phys. 23, 1112 (1984) and references cited therein.
- /7/ E.W. Becker, H.D. Falter, O.F. Hagen, P.R.W. Henkes, R. Klingelhofer, H.O. Moser, W. Obert, I. Poth, Fusion Technology, Pergamon Press, Oxford, 1979, p. 331.
- /8/ H.O. Moser, KfK 4068, 1986; H.O. Moser and B. Krevet, J. Appl. Phys. 58, 642(1985).
- /9/ Y. Chanut, J. Martin, R. Salin, and H.O. Moser, Surface Science 106, 563(1981).
- /10/ J.P. Thomas, P.E. Filpus-Luyckx, M. Fallavier, and E.A. Schweikert, Phys. Rev. Lett. 55(1), 103(1985); E.A. Schweikert, P.E. Filpus-Luyckx, J.P. Thomas, and M. Fallavier, J. Trace and Microprobe Techniques 2, 319(1984-1985).
- /11/ P.R.W. Henkes, U. Pfeiffer, Int. J. Mass Spectrom. Ion Phys. 52, 43(1983).

- /12/ M. Chevallier, A. Clouvas, H.J. Frischkorn, M.J. Gaillard, J.C. Poizat, and J. Remillieux, to be published in Z. Phys. D.
- /13/ G. Haas, P.R.W. Henkes, M. Keilhacker, R. Klingelhofer, and A. Staebler, Proceedings of the 3rd Symposium on Plasma Heating in Toroidal Devices, International School of Plasma Physics, Varenna, Italy, edited by E. Sindoni (Bologna Ed. Compositori, Italy, 1976).
- /14/ E.W. Becker, O.F. Hagen, P.R.W. Henkes, W. Keller, R.Klingelhofer, B. Krevet, and H.O. Moser, Nucl. Eng. Design 73, 187(1982); B. Krevet and H.O. Moser, Surface Science 156, 1020 (1985).
- /15/ S.H. Be and K. Yano, Rev. Sci. Instrum. 55,1928(1984).
- /16/ H.O. Moser, submitted to AIAA Journal.
- /17/ E.W. Becker, K. Bier, W. Henkes, Z. Phys.146, 333(1956).
- /18/ O.F. Hagen, in Molecular Beams and Low Density Gas Dynamics, ed. by P.P. Wegener (Marcel Dekker, New York, 1974); O.F. Hagen, Surface Science 106, 101 (1981).
- /19/ W. Henkes, Z. Naturforschg. A 16, 842(1961); W. Henkes, V. Hoffmann, F. Mikosch, Rev. Sci. Instrum. 48, 675-681 (1977).
- /20/ W. Paul, H.P. Reinhard, U. von Zahn, Z. Phys. 152, 143-182 (1958).
- /21/ H. Klein, M. Dähne, H. Deitinghoff, A. Gerhard, K.D. Halfmann, P. Junior, K. Langbein, R.W. Müller, J. Müller, W. Neumann, A. Schempp, A. Schönlein, Symp. on Accelerator Aspects of Heavy-Ion Fusion, March 29-April 2, 1982, Darmstadt, GSI 82-8, 1982, p. 150.

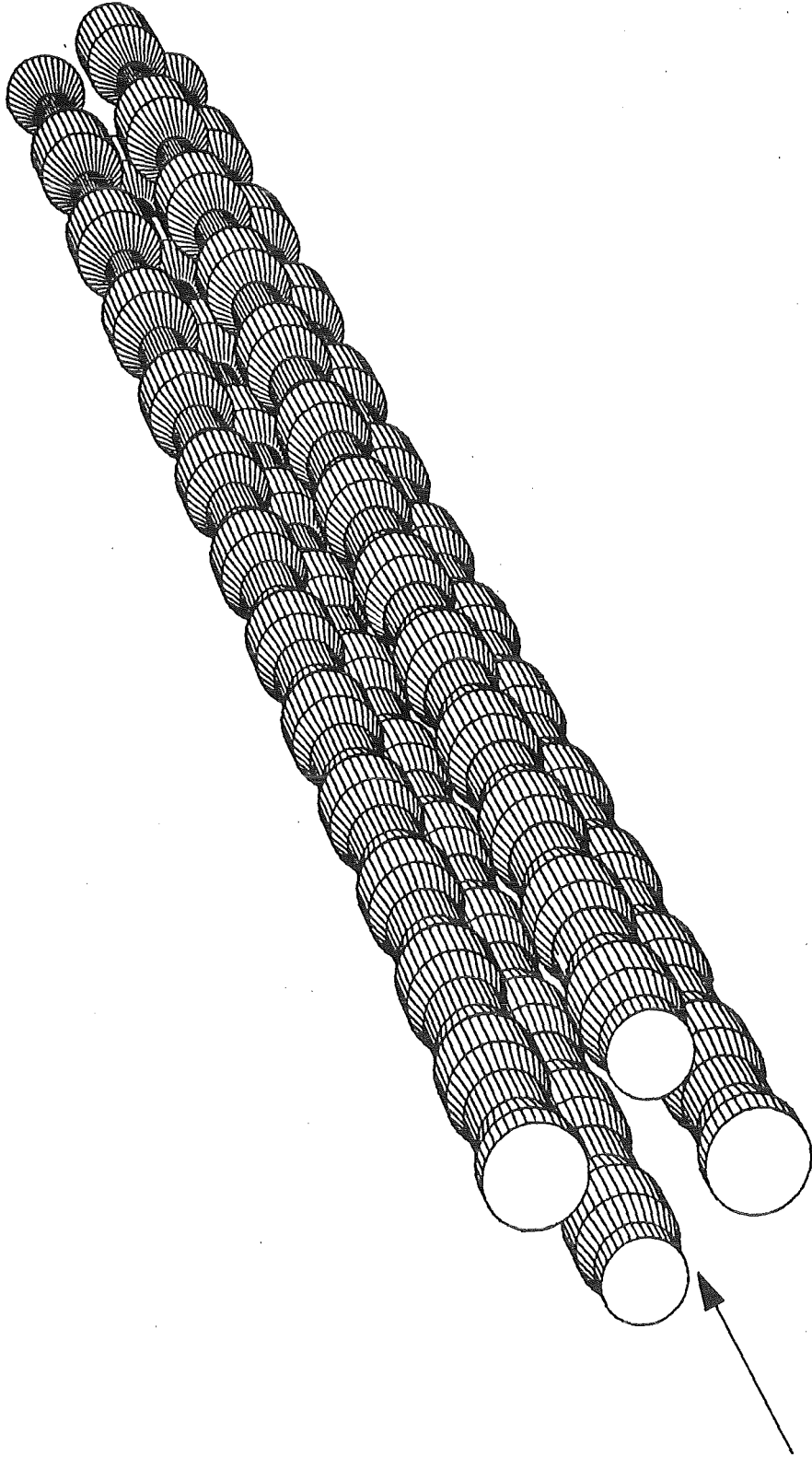


Fig. 1: Schematic of RFQ electrodes.

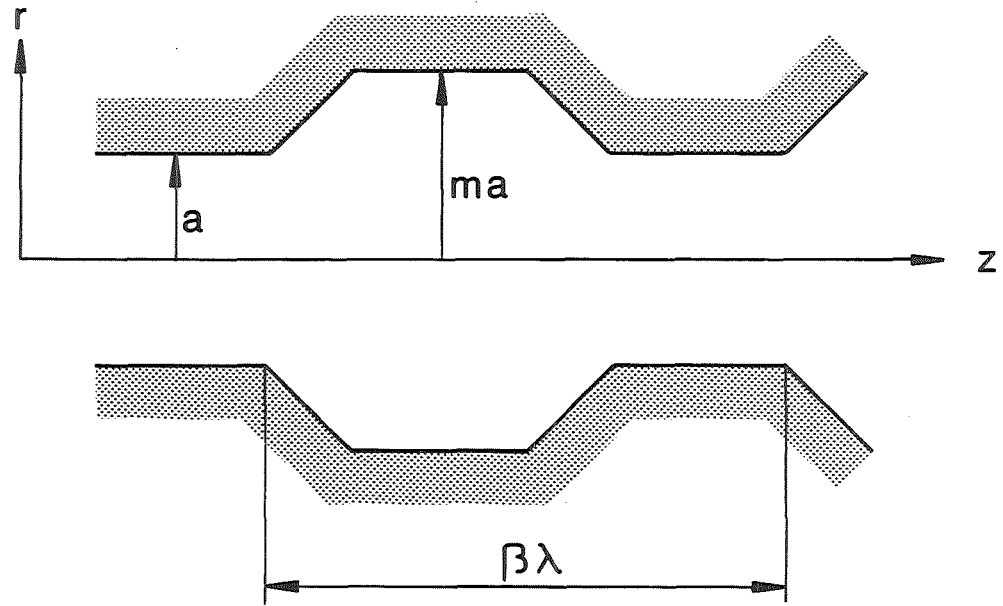


Fig. 2: Symbols characterizing the RFQ structure.

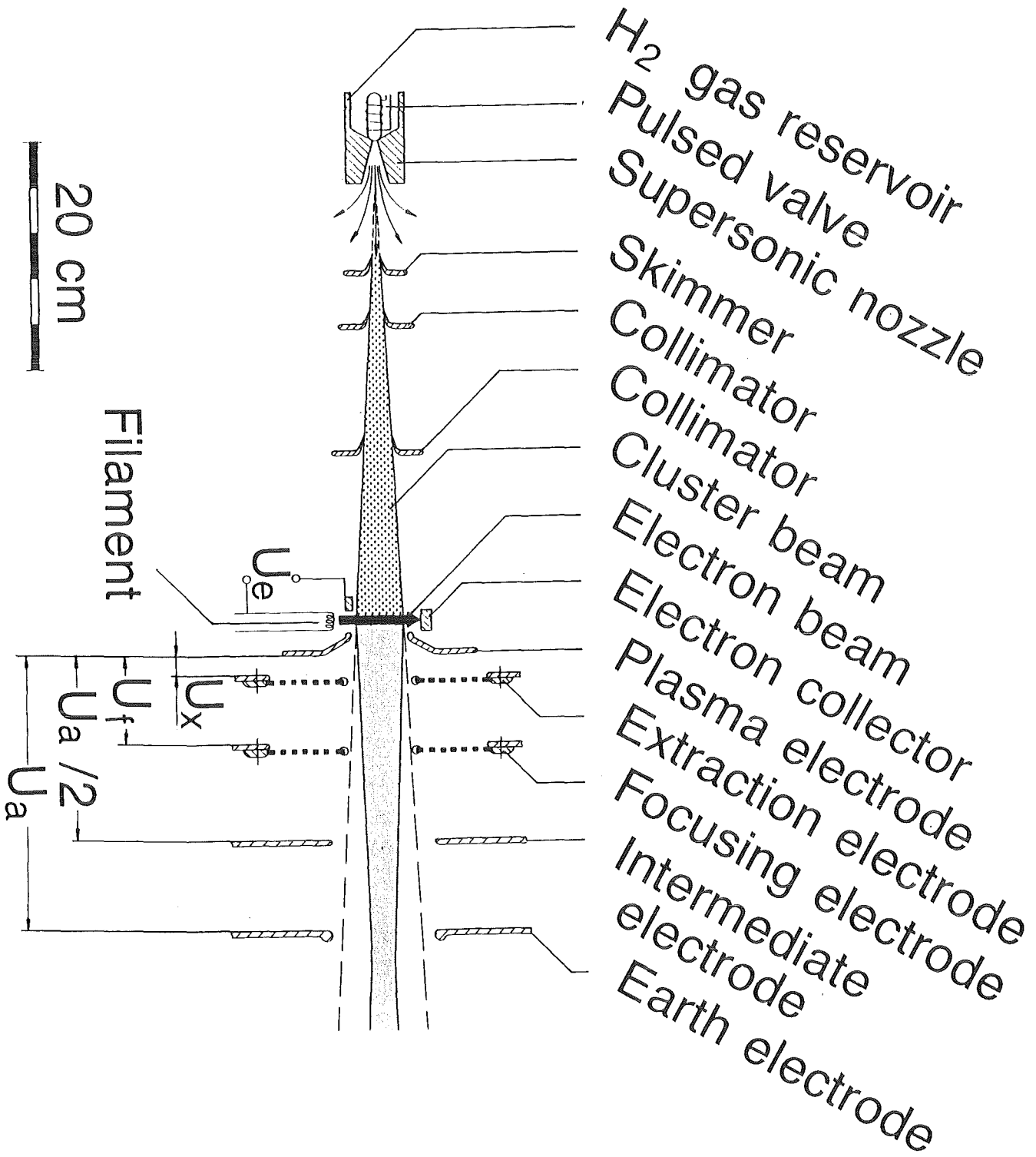


Fig. 3: Schematic of a cluster-ion source. Electrostatic acceleration electrodes are also shown.

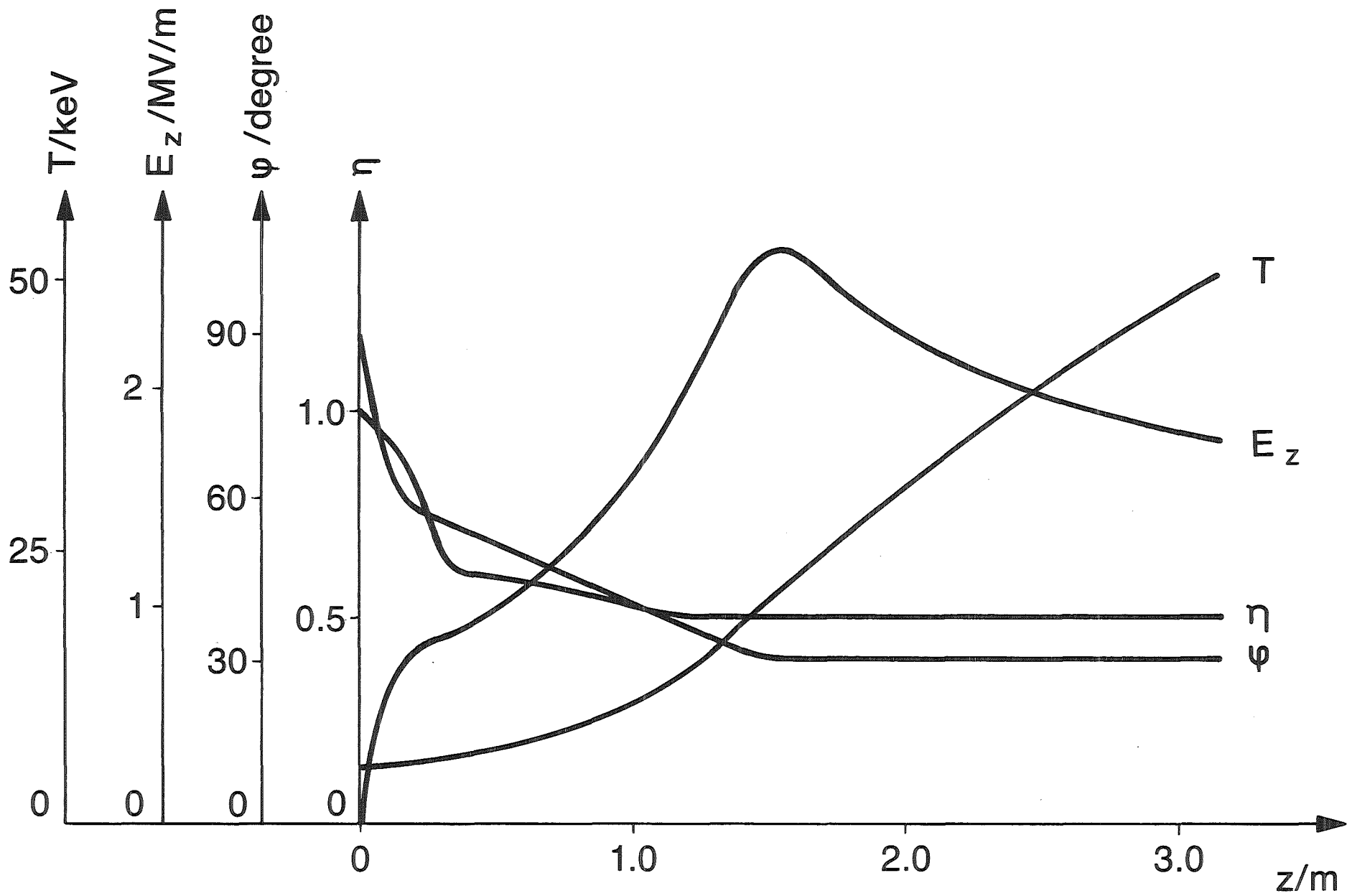


Fig. 4: Kinetic energy T , accelerating field strength E_z , phase ϕ , and transmission η versus the position z in the 3.15 m long RFQ.

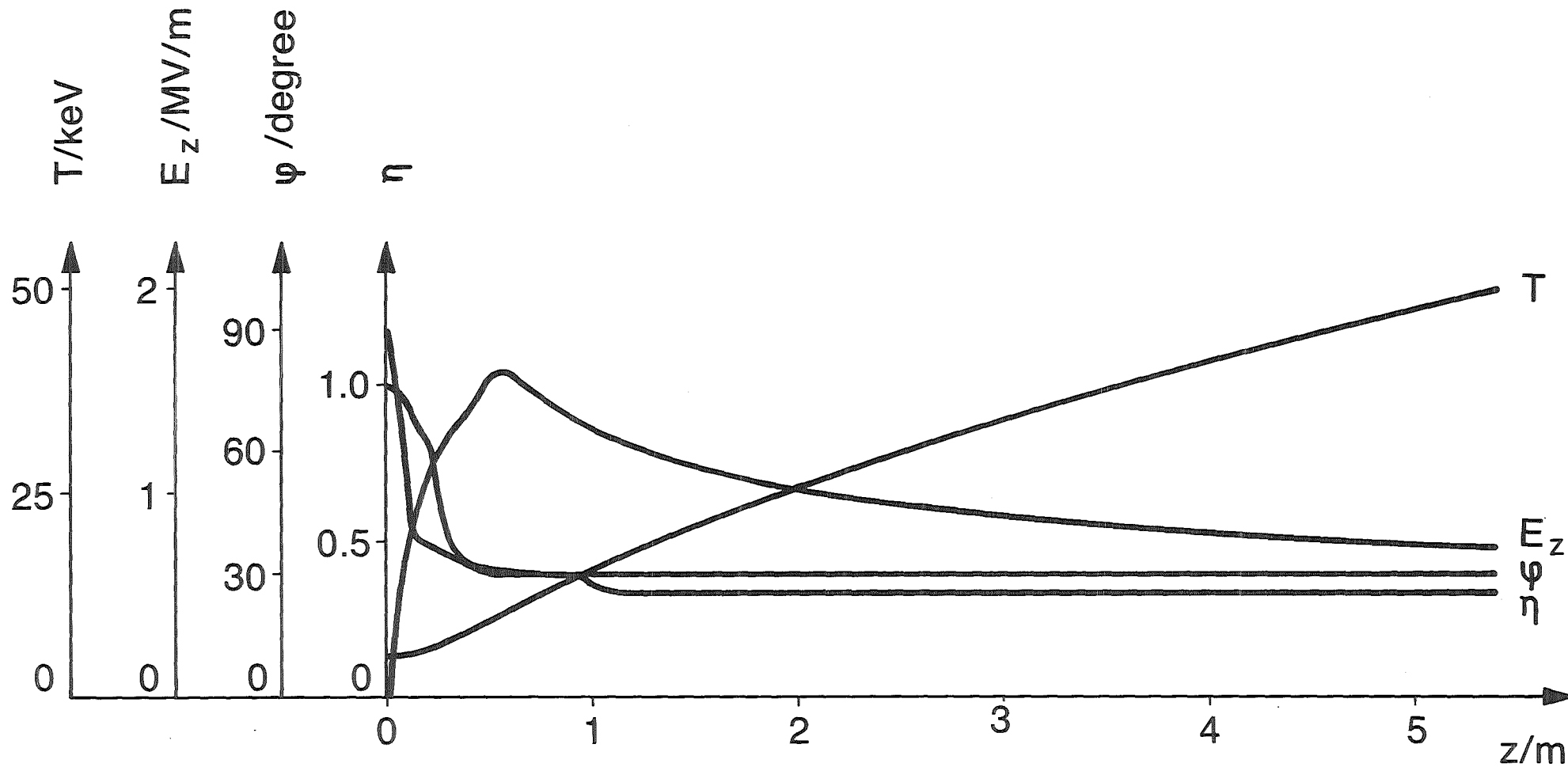


Fig. 5: Kinetic energy T , accelerating field strength E_z , phase ϕ , and transmission η versus the position z in the 5.43 m long RFQ.

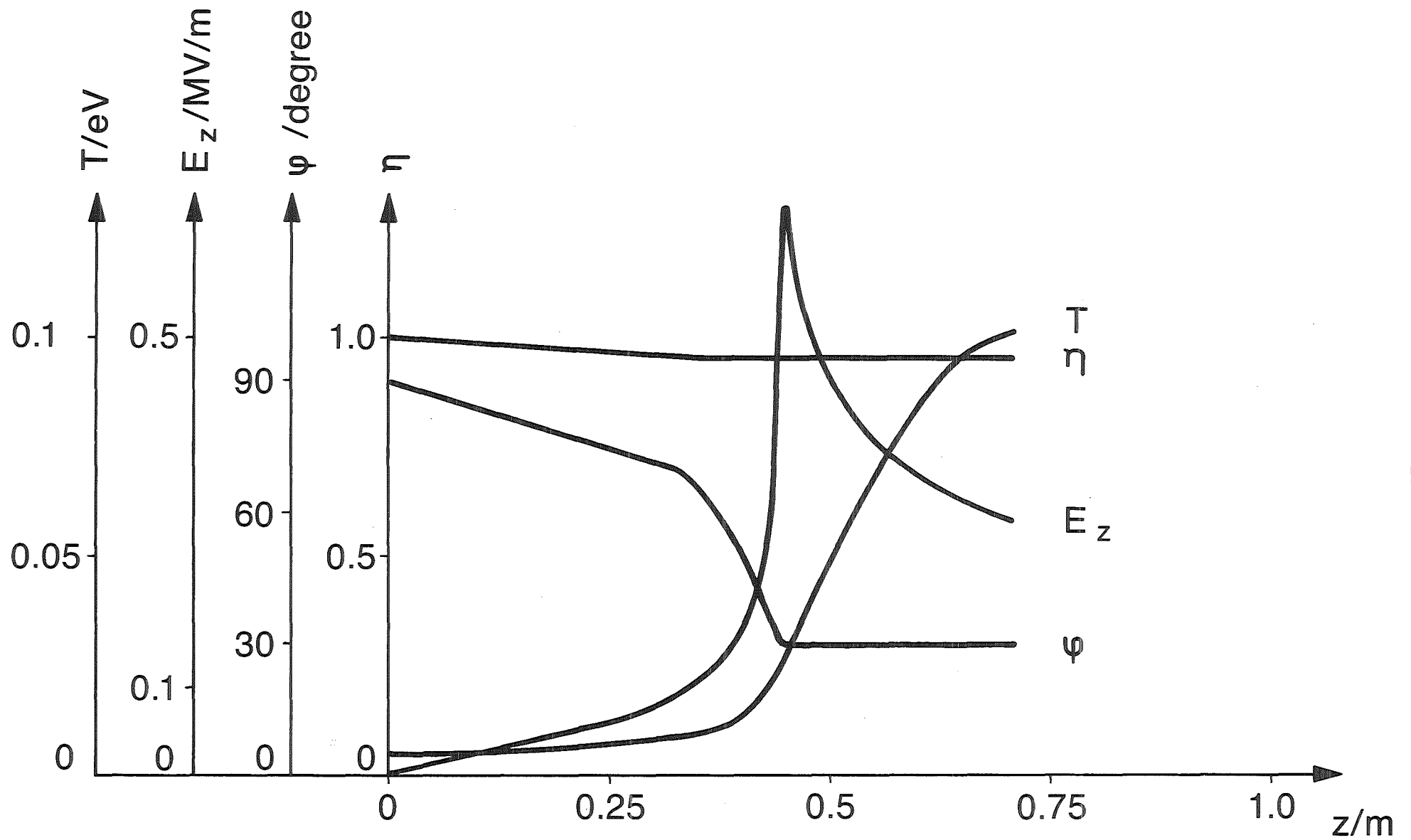


Fig. 6: Kinetic energy T , accelerating field strength E_z , phase ϕ , and transmission η versus the position z in the 0.71 m long RFQ.

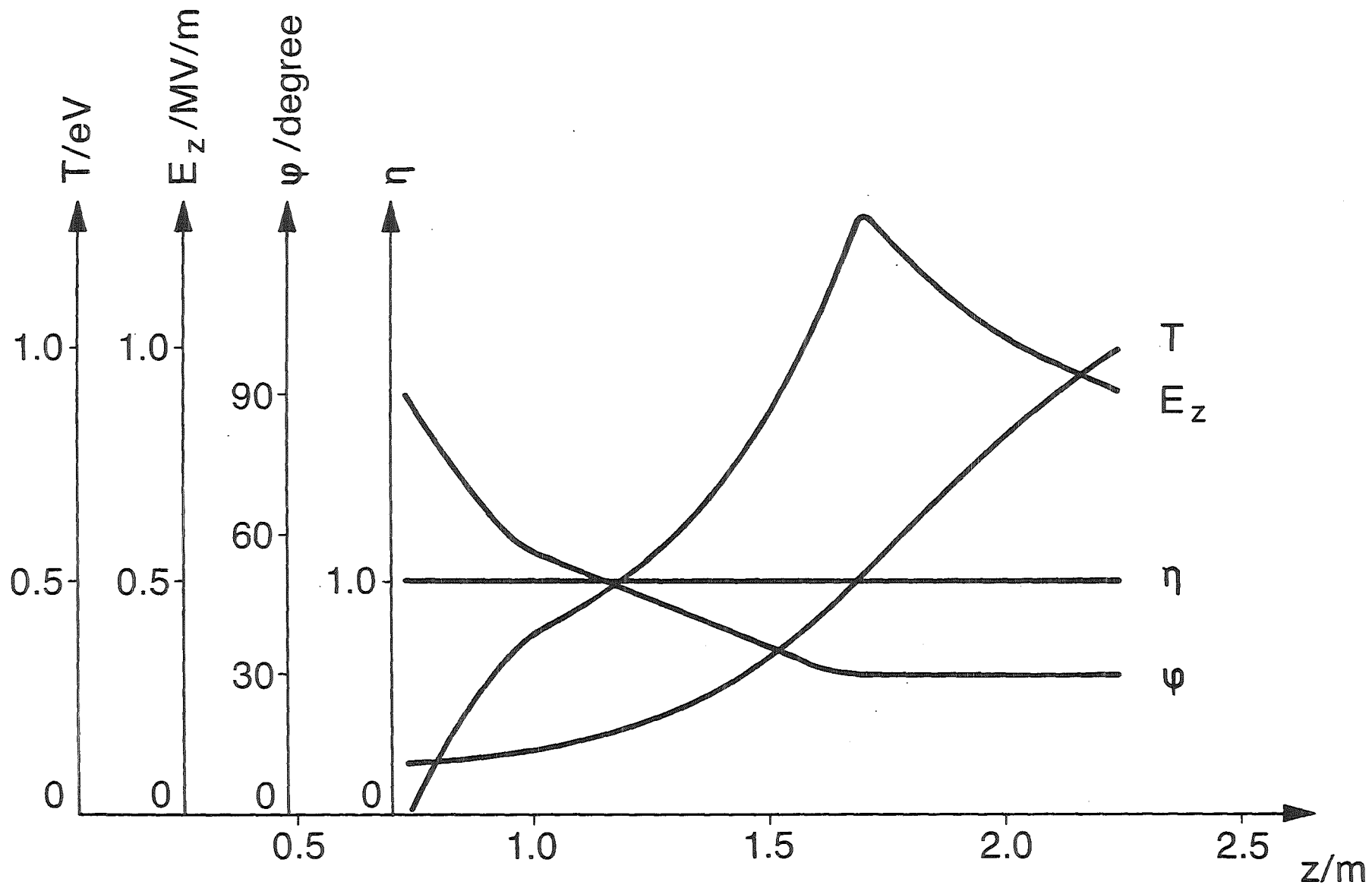


Fig. 7: Kinetic energy T , accelerating field strength E_z , phase ϕ , and transmission η versus the position z in the 1.6 m long RFQ.